Computer-aided diagnosis of head and neck lesions from non-Gaussian diffusion MRI signal patterns

Mami Iima[1], Akira Yamamoto[1], Denis Le Bihan[2,3], Shigeru Hirano[4], Ichiro Tateya[4], Morimasa Kitamura[4], and Kaori Togashi[1]

[1]Department of Diagnostic Imaging and Nuclear Medicine, Graduate School of Medicine, Kyoto University, Kyoto, Kyoto, Japan, [2]Human Brain Research Center, Graduate School of Medicine, Kyoto University, Kyoto, Kyoto, Japan, [3]Neurospin, CEA-Saclay Center, Gif-sur-Yvette Cedex, France, [4]Department of Otolaryngology, Head and Neck Surgery, Graduate School of Medicine, Kyoto University, Kyoto, Kyoto, Japan

Target audience: Scientists and clinicians interested in diffusion MRI with application to cancer

Introduction: Diffusion MRI (dMRI) has been widely used for the diagnosis and monitoring of cancers in many organs, including head and neck (1). Beyond simple ADC, non-Gaussian diffusion parameters (e.g. mean diffusion, ADCo, and kurtosis, K) provide important information on tissue microstructure (2-4). Accurate estimation of such parameters requires time-consuming fitting the dMRI signal with biophysical models (eg; kurtosis model), which in turn requires acquisition of images with a large range of diffusion sensitization (so called b values), resulting in long acquisition times. To cut on acquisition and processing times we have implemented an algorithm which enables automatic classification of tumor types (i.e. benign or malignant) directly based on the diffusion signal pattern ("signature") obtained from a very small set of "key b values", without actually estimating diffusion parameters. This "signature" algorithm has been evaluated in a series of patients with head & neck tumors.

Theory: Based on the IVIM/Kurtosis model (4) the dMRI signal can be modeled as: $S(b)=[S_0^2\{f_{IVIM}\exp(-bD^*) + (1- f_{IVIM})\exp[-bADC_0+(bADC_0)^2K/6]\}^2+NCF]^{1/2}$ [1]

where S_0 is the theoretical signal acquired at b=0, f_{IVIM} the (T1,T2-weighted) volume fraction of incoherently flowing blood in the tissue, D* the pseudo-diffusion coefficient associated to the IVIM effect, ADC_0 the virtual ADC which would be obtained when b approaches 0, K the kurtosis parameter and NCF (noise correction factor) a parameter which characterizes the "intrinsic" non-Gaussian noise contribution within the images (4).

Using typical values for fIVIM, ADCo, K and D* for malignant and benign lesions (4), typical differences in signals, $dS_{M,B}(b)=[S_{M,B}(b)- S_N(b)]/S_N(b)$ between malignant, S_M, and benign, S_B, tissue signals and a virtual "neutral" tissue signal, S_N, were calculated using Eq.[1]. The "key b values" (Lb (low b value) =150 or 200 and Hb (high b value) =1400 or 1500s/mm²) were chosen to minimize and maximize the difference between $dS_M(b)$ and $dS_B(b)$ (malignant lesions are characterized by high fIVIM, low ADCo and high K values, resulting in $dS_M>0$ and $dS_B<0$). A Signature index, SI(V), for a voxel signal, S_V, was defined as:

$SI(V) =\{\max([dS_V(Hb)-dS_V(Lb)]/[dS_M(Hb)-dS_M(Lb)],0) - [\max(dS_V(Hb)-dS_V(Lb)]/[dS_M(Hb)-dS_M(Lb)],0)\}$ [2]

SI>0 for malignant tissues (1 for typical malignant), SI<0 for benign tissues (-1 for typical benign) and SI=0 for a neutral (undetermined) tissue. The SI scale was further linearly scaled (Sindex=(SI+1)*25+25) to be centered at 50, so that Sindex=75 for a typical malignant tissue and Sindex=25 for a typical benign tissue. For normal tissues Sindex~ 0-20, while in very malignant tissues Sindex>100.

Material and Methods: This IRB approved prospective study included 46 (27 malignant/19 benign) patients suspected of head and neck tumors. Head and neck MRI was performed using a 3-T system (Skyra; Siemens AG) equipped with a dedicated 16-channel head and neck coil. The following images were obtained after localizers were acquired: 1. As the image quality of dMRI for head and neck lesion suffers from severe image distortion due to susceptibility artifact, a read-out segmented EPI (RS-EPI) sequence combined with GRAPPA parallel acquisition and 2D-navigator-based reacquisition was used (5,6) with the following parameters: 7 b values of 0, 100, 200, 500, 1000, 1500, 2000 sec/mm^2 or 9 b values of 0, 75, 150, 300, 600, 1000, 1400, 1800, 2200 sec/mm^2; repetition time/echo time; 2,000/17 ms; FOV: 220×220 mm^2; matrix: 148×148; slice thickness: 5.0 mm; 5 readout segments, parallel imaging factor 2, bandwidth 938 Hz/Px, echo spacing: 0.36 ms and scan time: 5 min 8 sec; 2. T1-weighted image: matrix size 256, FOV 180 mm x 180 mm, section thickness 4.0 mm; 20 sections without gap, TR/TE 700/12 ms. 3. 2The processing algorithm was implemented in Matlab (Mathworks, Natick, MA) and comprised the following steps: 1. Calculation of the the Signature index from manually or automatically drawn ROIs and on a voxel-by-voxel basis (from b=150/200 and 1400/1500 signals); 2. 3D clustering to remove spurious or isolated voxels and interpolation. The algorithm outputs consisted in statistics at ROI level (mean and standard-deviation of Sindex within the lesion, indices of lesion malignancy and heterogeneity, respectively, and a malignant charge taking into account the lesion volume with Sindex>50), color-encoded maps and 3D renderings of the lesion based on the voxel-by-voxel Sindex. A ROC analysis of the Sindex was performed to assess the algorithm performance on our patient series. Parametric maps of IVIM and diffusion parameters (fIVIM, ADCo and K) were also calculated, fitting the dMRI signal using all b values (4) with Eq.[1] for comparison purposes.

Results: Examples of lesion Sindex and parametric maps are shown in Fig.1 (malignant carcinoma of gingiva) and Fig.2 (benign schwannoma).

The histogram reflects the S-index distribution within the lesion (Smedian for carcinoma was 66.0, for schwannoma was 14). Parametric maps of ADCo, K and f_{IVIM} are also shown to illustrate tumor heterogeneity. Low ADCo/high K/high fIVIM are observed in gingival carcinoma, in contrast, schwannoma in fig. 2 shows combination of high ADCo/low K. low-moderate fIVIM.

The overall performance (AUC) of S-index for the study was 0.89 (sensitivity 88.9%; specificity 84.2%; PPV 88.9%, and NPV 84.2%), higher than AUC for ADCo, K, fIVIM (0.85, 0.83, 0.58, respectively.)

Fig.1

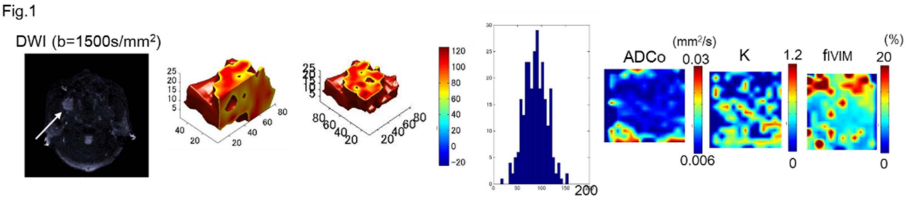

Fig.2

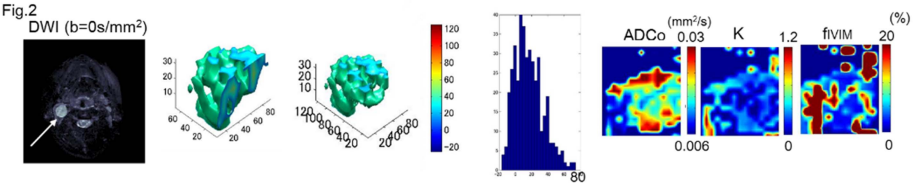

Anatomical image **S-index 3D rendering** **S-index histogram** **Parametric maps**

Discussion: This computer-assisted diagnostic algorithm, especially S-index, has enabled to differentiate malignant and benign lesions with relatively high AUC. Amount of distortion was remarkably decreased with RS-EPI, which allowed more cases to be analyzed. In addition, small lesions benefitted from a 3D cluster analysis, increasing voxel counts. An important feature of the Sindex is that only key b values are required (1 low and 1 high key b value) potentially resulting in short acquisition and processing time (the many b values used in this study was motivated by the quantitative estimation of IVIM/diffusion parameters for comparison purposes). Inspection of Sindex maps and 3D rendering usely showed sometimes the presence of a necrotic or cystic parts within the lesion, as in Fig.1. This finding strongly suggests the need to assess lesions taking into account their 3D structure, rather than at a global ROI (or even slice) level.

Conclusion: Head and neck lesions could be successfully characterized based on signature patterns of their dMRI signals without the need to calculate diffusion derived parameters. Signature patterns tissue recognition could be achieved from only 2 "key b values", resulting in a significant gain in acquisition and processing speed. Adding 1 or 2 more very low" key b values" could also allow vessel recognition from the IVIM effect. Although more work remains for further development and validation, this computer-assisted tool has the potential to give a semi-automatic diagnosis of head and neck lesions with high accuracy without the need for contrast agents, an important benefit for patients exposed to the risk of Nephrogenic Systemic Fibrosis (NSF). Furthermore, the diagnostic maps may provide guidance for accurate biopsy location. This approach is also under investigation for the diagnosis of breast, prostate, pancreas and lung cancer lesions.

References: (1) Chawla S. et al. Future Oncol. 2009;5;959-975. (2) Chabert S et al. Proceedings of the 12th Annual Meeting of ISMRM, Kyoto, Japan, 2004, p.1238. (3) Jensen JH et al. NMR in Biomedicine. 2010;23:698-710. (4) Iima M. et al. Invest Radiol. 2014 Sep 25. [Epub ahead of print] (5) Iima M. et al. AJNR 2012;33:1321-1325. (6) Koyasu S. et al. European Radiology 2014 Aug 13. [Epub ahead of print]